Dimeric 1,3-Phenylene-bis(piperazinyl benzimidazole)s: Synthesis and Structure-Activity Investigations on their Binding with Human Telomeric G-Quadruplex DNA and Telomerase Inhibit...

ARTICLE *in* JOURNAL OF MEDICINAL CHEMISTRY · MARCH 2012

Impact Factor: 5.45 · DOI: 10.1021/jm200860b · Source: PubMed

Journal of Medicinal Chemistry

Article

pubs.acs.org/jmc

Dimeric 1,3-Phenylene-bis(piperazinyl benzimidazole)s: Synthesis and Structure–Activity Investigations on their Binding with Human Telomeric G-Quadruplex DNA and Telomerase Inhibition Properties

Akash K Jain,[†] Ananya Paul,[†] Basudeb Maji,[†] K. Muniyappa,[§] and Santanu Bhattacharya*[,†,‡]

[†]Department of Organic Chemistry, Indian Institute of Science, Bangalore 560012, India

[‡]Chemical Biology Unit, Jawaharlal Nehru Centre for Advanced Scientific Research, Bangalore 560012, India

[§]Department of Biochemistry, Indian Institute of Science, Bangalore 560012, India

Supporting Information

ABSTRACT: Ligand-induced stabilization of G-quadruplex structures formed by the human telomeric DNA is an active area of research. The compounds which stabilize the G-quadruplexes often lead to telomerase inhibition. Herein we present the results of interaction of new monomeric and dimeric ligands having 1,3-phenylene-bis(piperazinyl benzimidazole) unit with G-quadruplex DNA (G4DNA) formed by human telomeric repeat d[$(G_3T_2A)_3G_3$]. These ligands efficiently stabilize the preformed G4DNA in the presence of 100 mM monovalent alkali metal ions. Also, the G4DNA formed in the presence of low concentrations of ligands in 100 mM K^+ adopts a highly stable parallel-stranded conformation. The G-quadruplexes formed in the presence of the dimeric compound are more stable than that induced by the corresponding monomeric counterpart. The dimeric ligands having oligo-oxyethylene spacers provide much higher stability to the preformed G4DNA and also exert significantly higher telomerase inhibition activity. Computational aspects have also been discussed.

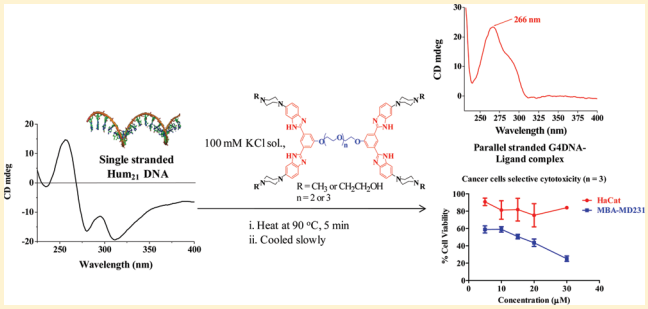

INTRODUCTION

A characteristic feature of the most biological polymers is their ability to fold into specific three-dimensional structures under physiological ionic conditions, and these structures are functionally definitive. The telomeric DNA consists of simple tandem repeats of guanine (G)-rich sequences, which are typified by the hexanucleotide d(5′-TTAGGG)$_n$ in vertebrates.[1,2] In eukaryotes, the telomere length of the repeat TTAGGG is in the range of 5–15 kb. In this region of telomeric DNA, the tandem repeats of the G-rich sequences fold into the G-quadruplex structures. All G4DNA structures contain a basic repeating and stacking motif, the G-quartet structure, which is formed by the four guanine bases and is held in a plane by Hoogsteen type hydrogen bonds.[3−6] Telomerase, a ribonucleoprotein complex of about 170 kDa, is up-regulated in about 80–90% of human tumors and is undetectable in most of the normal somatic cells.[7] The inhibition of telomerase activity overcomes the ability of cells to proliferate and leads to cell death. Telomerase enzyme is thus a highly attractive target for the selective anticancer therapy by the G-quadruplex-specific ligands.[4,8] In vitro experiments have shown that if the telomeric DNA is folded into G-quadruplex structures, it becomes insensitive to the elongation by telomerase.[8,9]

The intracellular concentrations of K^+ and Na^+ in animal cells are up to 150 and 15 mM, respectively.[10] Structure of the human telomeric G4DNA in Na^+ solution is antiparallel-stranded.[11] However, there has been a considerable debate regarding the exact structure of such DNA in a physiologically relevant K^+-rich environment. For example, the crystal structure of G4DNA in the presence of K^+ has been shown to be propeller-like and parallel-stranded.[12] However, this structure differs from the structure adopted under the physiological conditions. The favored conformation under the physiological environment was reported to be a hybrid structure having mixed parallel/antiparallel strands and three G-tetrads within the G4DNA.[13] Thus it was suggested that the crystal structure associated with the parallel-stranded conformation may not be relevant in the biologically active form.[14] Recently, a stable, basket-type, antiparallel stranded G4DNA structure having only two G-tetrad layers has been discovered in K^+ solution.[13d,15] The human telomeric DNA sequence adopts parallel-stranded conformation in K^+ solution in the presence of high concentrations of PEG.[16] This effect could be due to the dehydration of Hoogsteen hydrogen bonds caused by molecular crowding.[17] The conformation of the G-quadruplex DNA may be altered by an interaction with the G-quadruplex-specific ligands.[18] Most of the G-quadruplex DNA-specific compounds indeed have a central planar pharmacophore capable of binding to the guanine tetrads via $\pi-\pi$ stacking

Received: July 1, 2011
Published: March 27, 2012

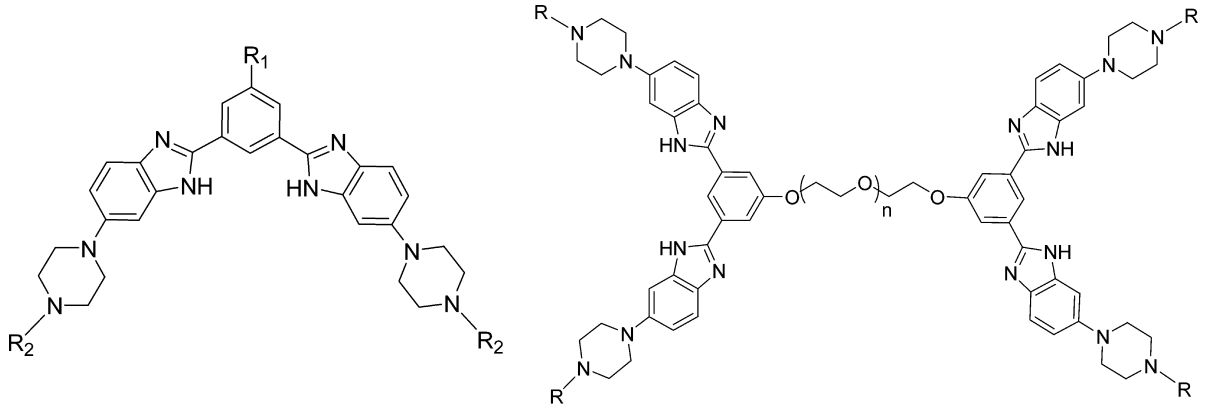

Figure 1. Chemical structures of the compounds used in this study.

Scheme 1[a]

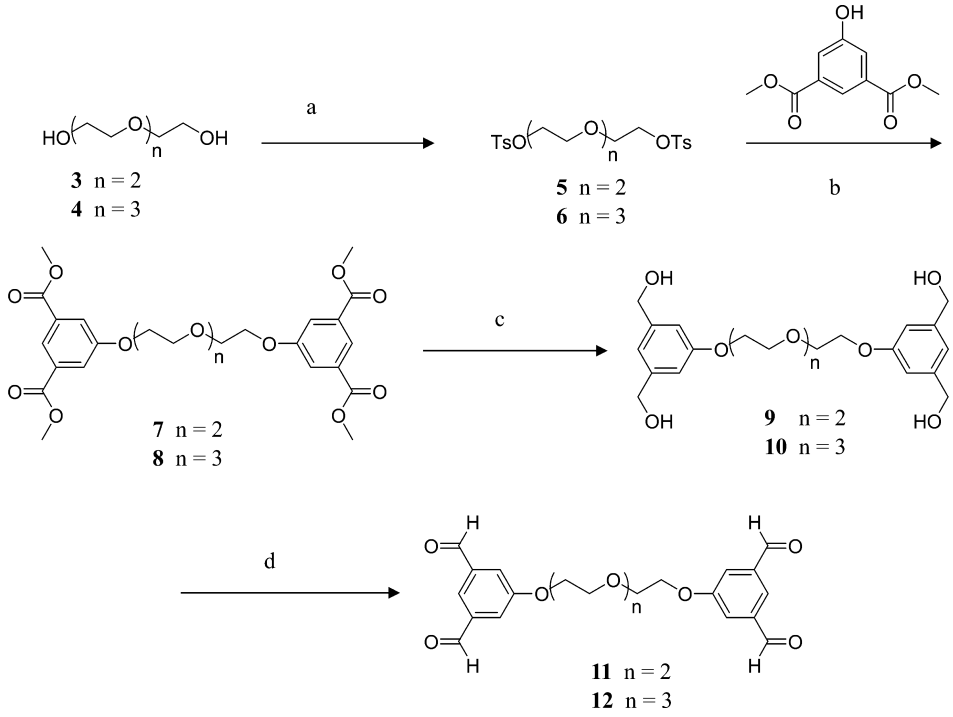

[a](a) *p*-TsCl, NaOH, THF/H_2O; (b) K_2CO_3, CH_3CN, reflux; (c) LAH, THF, rt; (d) PCC, DCM or DCM/THF, rt.

interactions. These also have side chains that can offer different modes of hydrogen bonding interactions directed toward the G-quadruplex loops and grooves.[19]

Bisbenzimidazole based Hoechst 33258 binds to the G4DNA assembled from the promoter region of human *c-myc*,[20] telomeric G-quadruplex[21] and some of its analogues have been found to stabilize triple-helical DNA at acidic pH.[22] Previously, we have reported the ability of small synthetic molecules based on benzimidazoles, some of which bind duplex DNA efficiently and few others inhibit the topoisomerase activity.[23] In this paper, we report the synthesis of a series of monomeric and dimeric derivatives to elucidate the minimum structural prerequisites and the ability of a molecule containing the dimeric motif to act as a potent G4DNA stabilizer. Indeed the dimeric forms of DNA targeting ligands are worthwhile for their design and synthesis. However, only a couple of studies are known where such ligands have been evaluated toward their binding of G4DNA. Recently, some dimeric G-quadruplex ligands, having higher quadruplex affinity than the corresponding monomeric ligands, have been developed. BRACO19 based dimers were found to have lower IC_{50} values for telomerase inhibition,[24] and dimeric ligands having macrocyclic hexaoxazole units were found to have lower IC_{50} values for G-quadruplex stabilization as determined by PCR stop assay.[25] However, these studies did not examine the preferred structure

dx.doi.org/10.1021/jm200860b | *J. Med. Chem.* 2012, 55, 2981−2993

of the G4DNA–ligand complex under the physiological environment.

We report herein the G4DNA formation by human telomere sequence $d[G_3(TTAG_3)_3]$ (abbreviated as Hum_{21}), its stabilization and structural alteration by six ligands having 1,3-phenylene-bis (piperazinyl benzimidazole) unit (monomeric ligands **1a** and **1b** and dimeric ligands **2a–2d**) (Figure 1). The central unit of these molecules is "V"-shaped, which has been shown to possess higher selectivity for the G4DNA than the corresponding linear isomeric ligands.[26] Monomeric ligands **1a** and **1b** have already been shown to stabilize and alter the topology of the G4DNA formed by the DNA sequence $d(T_2G_4)_4$, a telomeric repeat from *Tetrahymena thermophilia*.[27] Importantly, these compounds have >100 times greater affinity for the G4DNA than the AT-rich duplex DNA. Furthermore, these ligands induce G4DNA formation in the absence of any added cations.[27] The intrinsic fluorophoric properties of these ligands make the evaluation of their G-quadruplex binding properties particularly convenient. Therefore, we have developed the corresponding dimeric compounds and investigated in detail their abilities to stabilize G4DNA (Hum_{21}) using a number of different ways. We present the results of these findings in this paper.

RESULTS AND DISCUSSION

Synthesis. The following considerations were made while designing suitable ligands for achieving high stabilization of the G4DNA. Bisbenzimidazole compounds are known to be permeable across cell and nuclear membranes and have been used widely in cytometry and chromosomal staining.[28] Compounds having "V"-shaped central planar core have high affinity toward the G4DNA.[26,27,29] Polyethylene glycol based polymers, e.g., have both hydrophilic as well as lipophilic properties. Hence incorporation of oligo-oxyethylene based linker units between two bisbenzimidazole pharmacophoric units would further increase its cell permeability and make it more biocompatible. PEG also has other biological relevance along with its anticancer properties.[30] Consequently, we have synthesized first a member of some monomeric ligand molecules having central "V"-shaped planar core and the corresponding dimers having variable lengths of oligo-oxyethylene linkers connecting each monomeric units.

Briefly, for the synthesis of dimers, the glycols **3** or **4** were converted into respective ditosylates, which were then reacted with 5-ethoxy-isophthalic acid dimethyl ester to give the respective tetraesters **7** and **8** in 85% and 86% yields, respectively. Each compound **7** and **8** was then separately oxidized using PCC to obtain the key tetraaldehydes **11** and **12** in 70% and 72% yields, respectively (Scheme 1). Tetraaldehydes **11** and **12** were then subjected to oxidative coupling with diamines **13** or **14**[27] in the presence of $Na_2S_2O_5$[31] to give the final dimeric bisbenzimidazoles (**2a–2d**) in 60–62% yields (Scheme 2). Corresponding monomeric ligands **1a** and **1b** were synthesized as described earlier.[27]

G-Quadruplex Formation. Monovalent ions, e.g., Na^+ and K^+, are known to induce and stabilize the G4DNA structures. Li^+ ions on the other hand induce the G4DNA formation, but they have very little effect on the G4DNA stability.[32] In Na^+ solution, the sequence $d[AG_3(T_2AG_3)_3]$ folds intramolecularly into a G-tetraplex DNA stabilized by three stacked G-tetrads which are connected by two lateral loops and a central diagonal loop, leading to an antiparallel geometry.[11] The favored conformation under a physiological K^+ environment has

Scheme 2

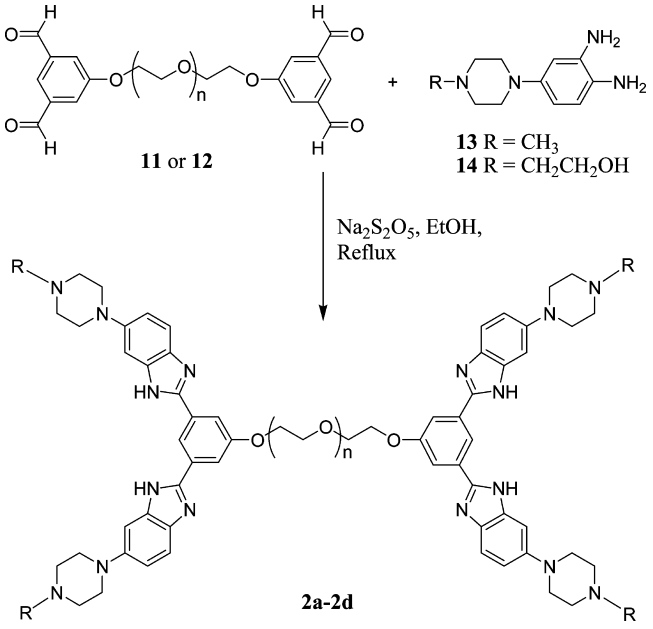

mixed parallel/antiparallel strands within the G4DNA.[13] We used three buffer systems, one having LiCl (10 mM sodium cacodylate having 100 mM LiCl and 0.1 mM EDTA, pH 7.4) and other two were made of either NaCl or KCl salts (10 mM Tris-HCl having 100 mM of either NaCl or KCl and 0.1 mM EDTA, pH 7.4). We used heat annealing conditions to form the G4DNA of the sequence $d[G_3(T_2AG_3)_3]$ (abbreviated as Hum_{21}, Materials and Methods). CD spectra obtained from the G4DNA formed by Hum_{21} in NaCl and KCl are similar to the reported ones (Figure 2).[16] G4DNA formed in KCl solution

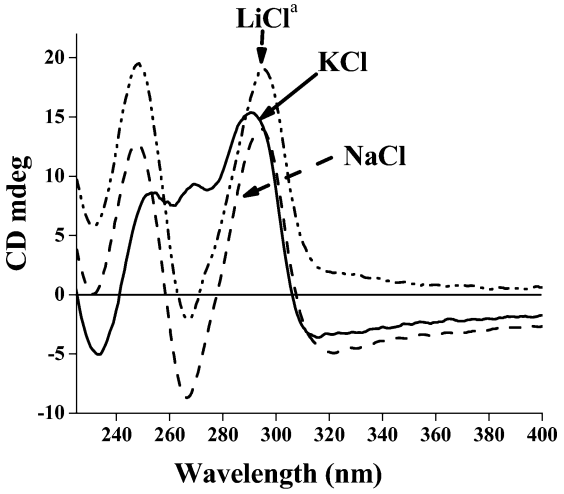

Figure 2. CD spectra due to G4DNA formed by human telomeric sequence Hum_{21} (4 μM strand concentration) in the presence of indicated ions (100 mM). [a]This contains 10 mM sodium cacodylate buffer and 100 mM LiCl.

has one small negative peak near 240 nm, one positive peak near 292 nm, and shoulders near 250 and 270 nm, similar to those reported for the human telomeric DNA in K^+ solution.[16] For the CD spectra of the G4DNA formed in LiCl buffer, the positions of the spectral peaks matched with those of the Na^+ quad but for the former the positive peaks at 295 and 245 nm

dx.doi.org/10.1021/jm200860b | J. Med. Chem. 2012, 55, 2981–2993

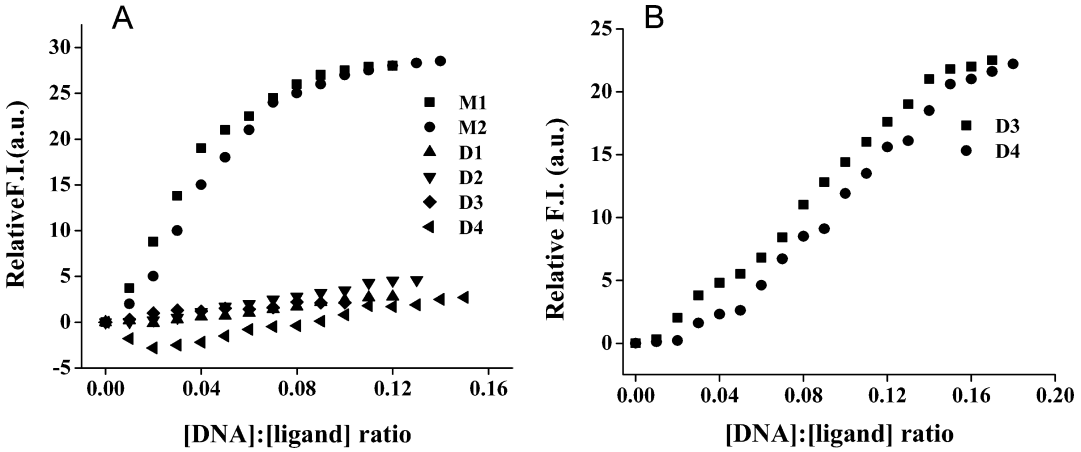

Figure 3. Relative increments in the fluorescence emission intensity due to the indicated ligands (400 nM of monomers or 200 nM of dimers) in LiCl buffer (10 mM sodium cacodylate having 100 mM LiCl and 0.1 mM EDTA, pH 7.4) (A) and in KCl buffer (10 mM Tris-HCl having 100 mM KCl and 0.1 mM EDTA, pH 7.4) (B). G4DNA formed by Hum_{21} was added from the stock of 4 μM strand concentration to the solution of the individual ligand in the cuvette.

were more intense while the negative peak at 264 nm was less intense than that of the latter (Figure 2).

Fluorescence and UV–Vis Titrations. Each of the monomeric and dimeric ligands displayed low fluorescence emission in Tris-HCl buffer having 100 mM LiCl (that also has 10 mM Na^+) at pH 7.4. During the fluorescence spectral titrations involving DNA, addition of preformed Hum_{21} G4DNA to either **1a** or **1b** induced significant enhancements in the fluorescence emission intensity, with the saturation point near [DNA]:[ligand] ratio = 0.1 or [ligand]:[DNA] ratio = 10 (Figure 3A). In contrast, the dimeric compounds showed considerably less increments in the fluorescence intensity upon addition of preformed Hum21 G4DNA under the same conditions. While only **2a** showed a moderate increment, ligands **2b** and **2c** showed much less increments in fluorescence than **2a**. In the case of **2d**, the fluorescence intensity first decreased and then increased slightly during titration with the above G4DNA (Figure 3A). These findings suggest that in LiCl solution, the monomeric ligands **1a** and **1b** bind with the preformed Hum_{21} G4DNA and stabilize the latter more effectively than their dimeric counterparts.

However, in 100 mM KCl solution, the dimeric ligands **2c** and **2d** showed significant fluorescence enhancements (Figure 3B). Saturation in the fluorescence emission occurred at [DNA]:[ligand] ratio = 0.16. In the case of the dimeric ligands, the two monomeric fluorescent ligand units are connected by an oligo-oxyethelene linker, which is capable to adopt a "crown ether" like conformation in the presence of alkali metal ion and transforms its conformation from a linear to a "hairpin"-like motif. Dimeric ligands **2a** and **2b** have a triethylene glycol based linker which is capable of forming a complex with the Li^+ ion and adopt a 12-crown-4 like structure (Figure S8, Supporting Information). Using fluorescence titrations, the association constant of binding of **2b** with Li^+ ion was found to be 5.5 ± 0.5 × 10^5 M^{-1} (method described in Supporting Information). The other dimeric ligands, **2c** and **2d**, possess a longer tetra-ethylene glycol based linker which is capable of forming a complex with Na^+ ion to adopt a 15-crown-5 like shape (Figure S8, Supporting Information). The association constant of binding of **2d** with Na^+ ion was found to be 2.3 ± 0.1 × 10^5 M^{-1}. Indeed, a computational study of **2b** and **2d** in presence of Li^+ and Na^+ ions respectively also suggests that the intervening oligo-oxyethylene linker chain adopts a crown ether type of structure in presence of these alkali metal ions in their energy minimized states (Figure S7, Supporting Information). How does the formation of a supramolecular complex with a metal ion influence their binding with the G4DNA? To answer this, we also carried out a control experiment in absence of preformed G4DNA at the identical salt concentration. In these circumstances, the ligands showed comparable fluorescence quenching in presence of Li^+ and Na^+ ions (Figure S9, Supporting Information). Ligands **2c** and **2d** did not, however, form supramolecular structures with K^+ ions. Under these circumstances, they showed efficient binding with the G4DNA in K^+ solution. However, a recent study shows that the formation of a ligand–metal supramolecular complex should not alter the activity of the ligand with the G4DNA or the duplex DNA.[33]

Next, we have determined the binding constants of the ligands with the preformed Hum_{21} G4DNA in KCl solution using the method described earlier.[26,27] Monomeric ligand **1b** provided higher stabilization of the G4DNA than **1a**, presumably because of the presence of an electron-donating ethoxy group (Table 1).[26] Among dimeric ligands, **2c** and **2d**, the one having longer tetraethylene glycol linker provided higher stabilization of the G4DNA than **2a** and **2b** having shorter linkers. Dimeric ligand **2d** exerted the highest stabilization (Table 1).

Table 1. Dissociation Constant (K_D) of All Four Compounds with Preformed Hum_{21} G4DNA Formed in KCl Buffer[a]

	K_D (10^7 M^{-1})
ligand	Hum_{21} G4DNA
1a	4.25 ± 0.1
1b	8.49 ± 0.2
2a	6.04 ± 0.2
2b	6.54 ± 0.6
2c	9.15 ± 0.6
2d	12.28 ± 0.3

[a]Binding assays were performed with preformed Hum_{21} G4DNA in 10 mM Tris-HCl, having 100 mM KCl and 0.1 mM EDTA buffer, at pH 7.3.

dx.doi.org/10.1021/jm200860b | J. Med. Chem. 2012, 55, 2981–2993

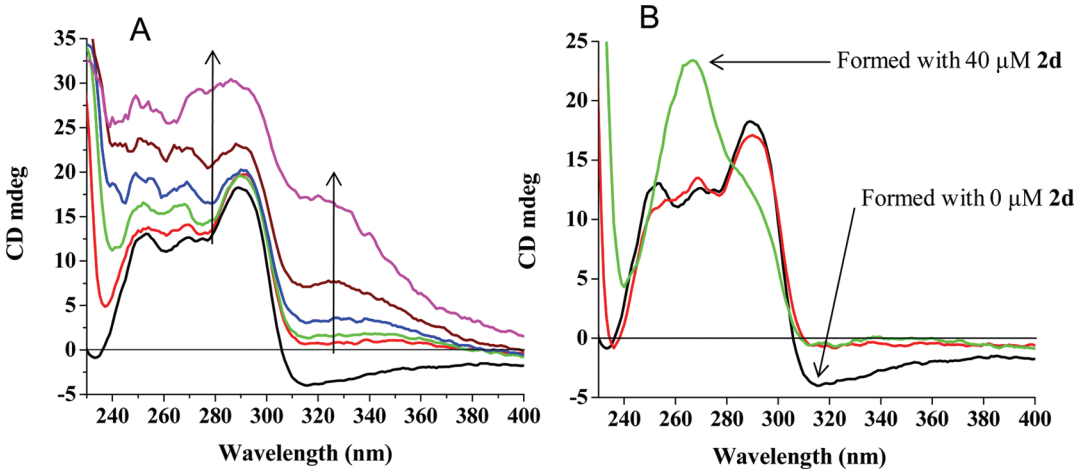

Figure 4. (A) CD titrations of the preformed Hum_{21} G4DNA (4 μM strand concentration) with increasing amount of **2d** (0, 20, 40, 60, 80, and 100 μM), respectively, in KCl buffer (10 mM Tris-HCl having 100 mM KCl and 0.1 mM EDTA, pH 7.4). (B) CD spectral profiles of the Hum_{21} (4 μM strand concentration) G4DNA formed in presence of 0, 20, and 40 μM of **2d** (heated at 90 °C for 5 min and then cooled slowly) in 100 mM KCl buffer.

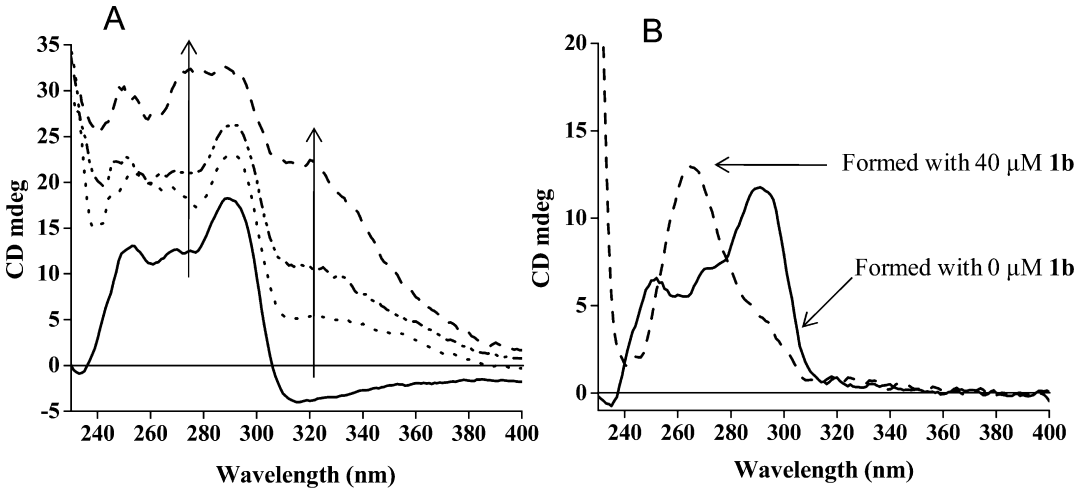

Figure 5. (A) CD titrations of the preformed Hum_{21} G4DNA (4 μM strand concentration) with increasing amount of **1b** (0, 40, 60, and 100 μM, respectively) in KCl buffer (10 mM Tris-HCl having 100 mM KCl and 0.1 mM EDTA, pH 7.4). (B) CD spectral profiles of the Hum_{21} (2 μM strand concentration) G4DNA formed in presence of 0 and 40 μM of **1b** (first heated at 90 °C for 5 min and then cooled slowly) in 100 mM KCl solution.

Circular Dichroism Spectroscopy. Next, we performed CD spectral titrations involving individual ligands with the preformed G4DNA formed in LiCl buffer (10 mM sodium cacodylate having 100 mM LiCl). No noticeable structural change was observed with **2a** and **2b** based on the CD spectral profiles (Figure S9, Supporting Information). But the positive peaks in the CD spectra at 245 and 295 nm became less intense, indicating some interaction of G4DNA with the ligands. With dimeric ligands having longer linker, i.e., **2c** and **2d**, the peak at 295 nm was found to be much less pronounced, suggesting their stronger interactions with G4DNA (Figure S10, Supporting Information).

Solution structure of K^+ stabilized G-quadruplex has significant biological relevance.[13d,14] Hence, we performed CD spectral titrations of preformed G4DNA in K^+ solution with **2d**. The peaks observed at 250, 270, and 292 nm in the CD spectra were a bit more intense and the negative band minimum around 232 nm started going up at lower concentrations of **2d** (Figure 4A) although the conformation of the G4DNA appeared to have remained invariant. Besides the planar G-quartet regions of the G4DNAs, there are also several grooves available for the interaction with a guest molecule.[34] Incidentally, we did not observe any isodichoric point in the CD spectral titrations, which could be due to the presence of more than one G-quadruplex conformations in solution. This was also consistent with the reported NMR spectrum of the 22-mer human telomeric sequence in K^+ solution. The NMR spectrum indicated existence of a broad envelope with some fine lines, implying the presence of multiple conformational isomers of the G4DNA.[13a] An induced CD signal (ICD) appeared near 330 nm above the [ligand]:[DNA] ratio of 15, which could be due to the interaction of the added ligand with the chiral grooves of the G4DNA. The side chains of the G4DNA binding compounds also have their role in groove binding.[35] Benzimidazole molecules are known to cause DNA aggregation and have been shown to undergo self-aggregation at higher concentrations.[27,36] At higher [ligand]:[DNA] ratio (particularly above r = 25), the ICD signal increased significantly and merged with the peak at 295 nm. Such an observation at high compound concentration is

dx.doi.org/10.1021/jm200860b | J. Med. Chem. 2012, 55, 2981−2993

possibly due to the formation of a distorted structure or owing to some pronounced aggregation of the ligands.[27]

But dramatic changes occurred in the CD spectral profile of the G4DNA formed in presence of **2d** in 100 mM K^+ solution. At [ligand]:[DNA] ratio = 5, the small positive peak at 245 nm in the CD spectra disappeared with the concomitant appearance of a shoulder and instead the small peak at 270 nm became more intense while the peak at 295 nm became less pronounced (Figure 4B). The shallow at 232 nm also became red-shifted to 237 nm. Interestingly, at [ligand]:[DNA] ratio of 10, all the three peaks merged to give a peak at 265 nm and a shoulder at 295 nm (Figure 4B). This profile is similar to the CD spectral profile of the parallel G-quadruplexes formed by human and many nonhuman telomere sequences.[16,37] The only difference is the presence of a shallow near 237 nm and not a negative peak. At higher [ligand]:[DNA] ratio (at [ligand]:[DNA] ratio = 50, i.e., 200 μM of **2d**), a distorted structure or pronounced aggregation was observed as it was in the case of the preformed G4DNA. We also examined the effect of monomer **1b** on the conformation of Hum_{21} quadruplex in 100 mM K^+ solution (preformed G4DNA and G4DNA formed in the presence of the compound) and obtained similar results as described in the case of **2d** (Figure 5).

These results suggest that the compounds **1b** and **2d** are capable of interacting with the preformed K^+-quad without causing any structural alteration. But these ligands are capable of directing the folding of randomly structured Hum_{21} sequence into the parallel-stranded G4DNA at low concentrations when the G-quadruplex is formed in 100 mM K^+ solution in presence of such compounds. Similar structural change was not, however, observed when G-quadruplex DNA was formed in 100 mM Na^+ solution in presence of **1b** and **2d** (Figure 6).

Thermal Denaturation. In thermal denaturation experiments, **1a** and **1b** showed characteristic melting curves upon monitoring the changes in the CD spectral maximum at 295 nm as a function of temperature. These melting profiles suggest significant stabilization (of 9.5 and 11.5 °C, respectively) of the preformed Hum_{21} G4DNA in 100 mM LiCl solution at [ligand]:[DNA] ratio of 5 upon binding with **1a** or **1b** (Figure 7A, Table 1). We have chosen LiCl solution because Li^+ folds telomeric DNA into (like Na^+) G4DNA but it does not stabilize the G4DNA structure on its own.[32] Therefore, this study allows one to have a good idea about the stabilization provided by any G4DNA interacting ligand. Electron-donating substituents in the ligands that interact with the G4DNA play an important role in the G4DNA stabilization. Many of the established G4DNA interacting ligands, e.g., berberine,[38] telomestatin,[39] dounomycin,[40] adrinamycin,[41] etc., contain functional groups with electron-donating character. Side chains of the G4DNA-specific ligands may also play an important role in the G4DNA stabilization.[27,35] Ligand **1b**, having an electron-donating ethoxy group at the phenyl ring and 2-hydroxyethyl group at the piperazine units, provide higher stabilization to the G4DNA than that of **1a** (Table 1), which possess an ethoxy group at the phenyl ring but only a methyl group at the piperazinyl rings. The benzimidazole hydrogens in such ligands may also play their role in the structural transition and consequent stabilization of the G4DNA.

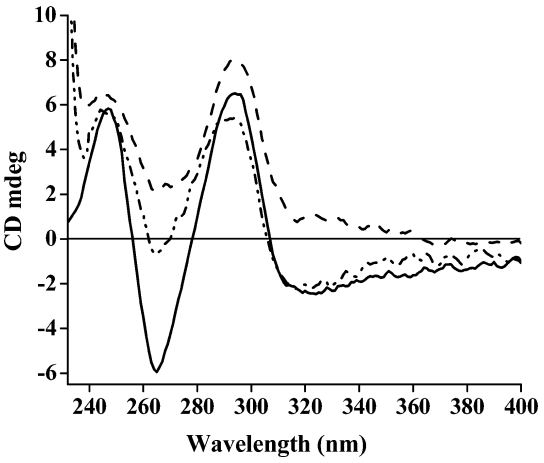

Figure 6. CD spectral profiles of the Hum_{21} (2 μM strand concentration) G4DNA without any ligand (solid line) and G-quadruplex DNA formed in presence of 20 μM of **1b** (dashed−dotted line) and **2d** (dashed line) (first heated at 90 °C for 5 min and then cooled slowly) in 100 mM NaCl solution.

When added to the preformed G4DNA in LiCl solution at [ligand]:[DNA] ratio = 5, the dimeric ligands **2c** and **2d** induced lesser stabilization (Table 2). The melting curves were not so cooperative (Figure S11, Supporting Information). This might be because of a complex formation between the ligand (having oligo-oxyethylene linker) and Li^+ ion, which was also evident from the fluorescence studies.

But interestingly, when the G4DNA was formed in presence of **2d** in LiCl solution (first heated at 90 °C for 5 min, and then allowed to cool slowly), it showed higher stabilization (13 °C, Table 2) with a characteristic melting curve (Supporting Information). The ligand **2d** might be able to occupy every possible binding site when single-stranded Hum_{21} starts folding in presence of the ligand into a G-quadruplex structure, leading a higher stabilization.

In 100 mM Na^+ solution, the Hum_{21} G4DNA has higher melting temperature (57 °C, Table 3) because of the stabilization provided by the Na^+ ions. To see the effect of ligands on the stability of the G4DNA in Na^+ solution, we used a higher [ligand]:[DNA] ratio of 10. Ligand **1b** and **2d** caused melting temperature increments of 11 and 14 °C respectively in Na^+ solution when monitored at 295 nm using CD spectroscopy as a function of temperature (Figure 7B, Table 3).

Taken together, the CD titrations and the thermal denaturation data indicate that although Li^+ and Na^+ ions are capable of forming complexes with the dimeric ligands (as evident from the fluorescence titrations), these ligands are able to bind strongly with the Hum_{21} G4DNA in the presence of such alkali metal ions, leading to the stabilization of the G4DNA. The binding is more favorable when the G-quadruplex structure was formed in presence of the dimeric ligands.

CD melting results were even more striking when performed in 100 mM K^+ solution. In fact, K^+ solution is biologically more relevant and K^+ ions form very stable G4DNA structures.[13−16] It is therefore difficult to measure the stabilization provided by a weak stabilizing ligand in K^+ solution. At [ligand]:[DNA] ratio =10, **1b** and **2d** provided less stabilization (6 and 9 °C, respectively, Figure 8, Table 4) with the preformed G4DNA in presence of K^+ ions. Stabilization was, however, significantly higher when the G4DNA was formed in presence of either ligand **1b** or **2d** at [ligand]:[DNA] ratio of 10 in 100 mM K^+ solution (14.5 and 16 °C, respectively, Figure 8, Table 4).

dx.doi.org/10.1021/jm200860b | J. Med. Chem. 2012, 55, 2981−2993

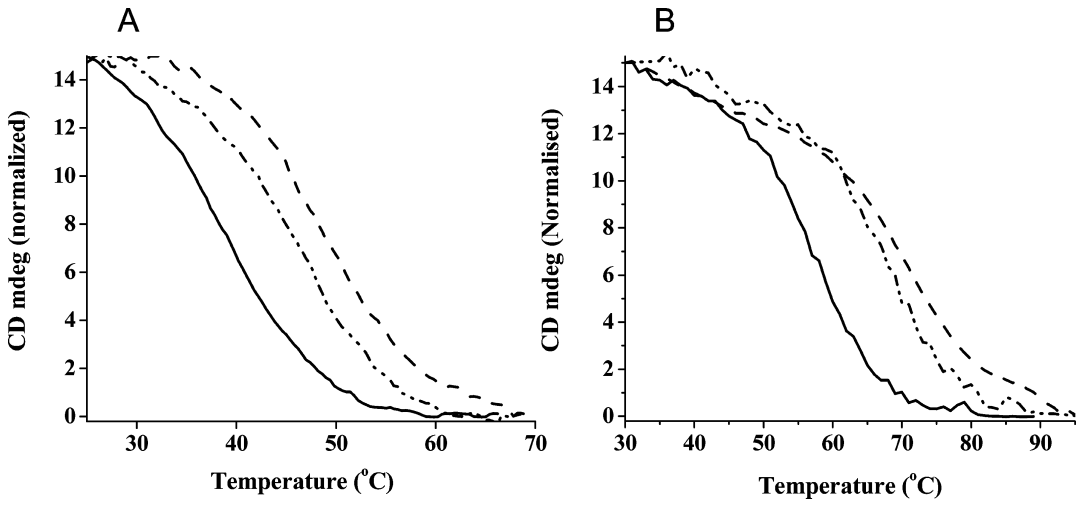

Figure 7. CD melting profiles (at 295 nm) of the preformed Hum_{21} G4DNA (2 μM, solid lines) and its complex with 10 μM of **1a**, (dashed−dotted line) and **1b**, (dashed line) respectively in LiCl buffer (10 mM sodium cacodylate having 100 mM LiCl and 0.1 mM EDTA, pH 7.4). (B) CD melting profiles (at 295 nm) of the preformed Hum_{21} G4DNA (2 μM, black) and its complex with 20 μM of **1b**, (dashed−dotted line) and **2d**, (dashed line) in NaCl buffer (10 mM Tris-HCl buffer having 100 mM NaCl and 0.1 mM EDTA, pH 7.4), respectively.

Table 2. Thermal Denaturation Temperatures (on the basis of DNA melting as probed by CD spectra) of Hum_{21} G4DNA (2 μM strand concentration) Formed in LiCl Buffer (10 mM sodium cacodylate having 100 mM LiCl and 0.1 mM EDTA, pH 7.4), and G4DNA Complexed Either with 10 μM ([ligand]:[DNA] ratio = 5) of the Indicated Ligand at 295 nm

entry	system	T_m °C[a]	ΔT_m °C[b]
1	Hum_{21}	37.5	
2	Hum_{21} + **1a**	47	9.5
3	Hum_{21} + **1b**	49	11.5
4	Hum_{21} + **2c**	45	7.5
5	Hum_{21} + **2d**	45.5	8
6	Hum_{21} + **2d**[c]	50.5	13

[a]The results are average of three experiments and are within ±0.5 °C of each other. [b]ΔT_m values were obtained from the difference in melting temperatures of the ligand bound and uncomplexed G4DNA. [c]For entry 6, G4DNA structure was formed in LiCl buffer (first heated to 90 °C for 5 min and then cooled slowly).

During the cooling event in KCl solution, Hum_{21} DNA alone did not form any specific DNA structure (Figure 8C). Cooling of the solution of Hum_{21} in the presence of either **1b** or **2d** resulted in G-quadruplex formation. However, there was evidence of hysteresis and the cooling curves were not superimposable with the heating curves. Reformation of G4DNA was more significant in case of **2d**.

Table 3. Melting Temperatures[a] of the Hum_{21} G4DNA Formed in NaCl Buffer and G4DNA Complexed with 20 μM of Indicated Ligands at ([ligand]:[DNA] ratio = 10)

entry	system	T_m °C	ΔT_m °C[b]
1	Hum_{21}	57	
2	Hum_{21} + **1b**	68	11
3	Hum_{21} + **2d**	71	14

[a]Changes in the circular dichroism spectral peak at 295 nm observed as a function of temperature using 2 μm stand concentration of DNA in 10 mM Tris-HCl, pH 7.4, having 100 mM NaCl and 0.1 mM EDTA. [b]ΔT_m values were obtained from the difference in melting temperatures of the ligand bound and uncomplexed G4DNA. The results are average of three experiments and are within ±0.5 °C of each other.

Electrophoresis. To examine whether these benzimidazoles trigger any topology change of the G-quadruplex DNA, we performed the electrophoresis of the 5′-^{32}P-end labeled preformed Hum_{21} G-quadruplex DNA in 100 mM KCl and G-quadruplex formed in the presence of either of **1b** or **2d** at different [ligand]:[DNA] ratios in 100 mM KCl solution. Under comparable conditions, electrophoresis was also performed using a dT_{20} marker. All the G4DNA bands formed expectedly showed considerably higher mobility than that of the dT_{20} ODN under identical conditions (Figure S12, Supporting Information). The preformed G4DNA complexed with **1b** displayed a similar mobility as that of the uncomplexed G4DNA, suggesting that there was no change in the topology of the G-quadruplex upon binding with **1b**. But the G4DNA formed in presence of either **1b** or **2d** have lower mobility than that of the preformed G4DNA, although the former possessed higher electrophoretic mobility than that of the dT_{20} ODN (Figure S12, Supporting Information). The gradual mobility shifts at higher [ligand]:[DNA] ratio in the case of **2d** may be due to the binding effect because **2d** has higher molecular weight (1323.975) than that of **1b** (MW = 610.34). However, the mobility of the **2d** bound G-quadruplex DNA is still higher than that of the dT_{20} ODN in any case. These results are consistent with those reported earlier for the G4DNA formed by Hum_{21}.[16] In the reported instance, both the hybrid G4DNA and the parallel G4DNA structure formed in molecularly crowded conditions (simulated by PEG in KCl solution) had higher mobility than that of the dT_{21} marker and the parallel G4DNA had the intermediate mobility between the hybrid G4DNA and the dT_{21} marker. Hence we believe that the mobility shifts observed in the case of G4DNA formed in presence of either **1b** or **2d** are due to the structural conversion and not due to any aggregation. If it would have been due to aggregation, then the mobility of the ligand−DNA complex would be much lower than that of the dT_{20} ODN. Also, as suggested by the CD spectroscopic data, the aggregation, if it occurs at all, would appear only beyond [ligand]:[DNA] ratio >25.

dx.doi.org/10.1021/jm200860b | J. Med. Chem. 2012, 55, 2981−2993

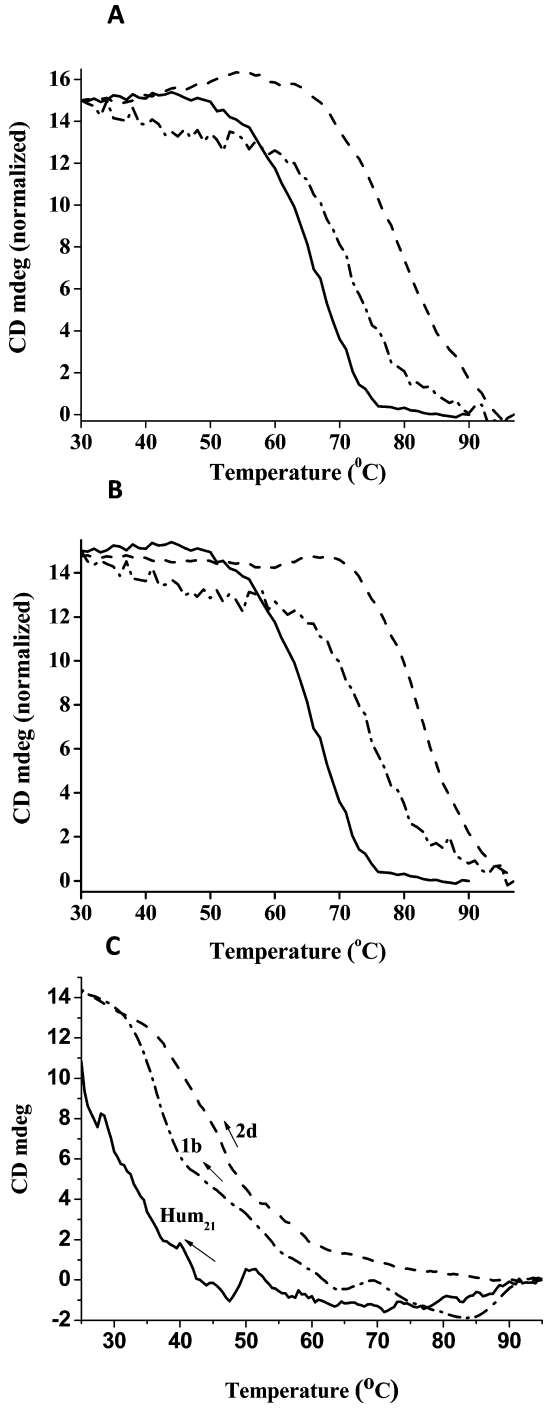

Figure 8. CD melting profiles of the Hum_{21} G4DNA alone (2 μM, solid line, at 292 nm) and its complex with 20 μM of **1b** (dashed–dotted line, A) and **2d** (dashed line, B), respectively, in KCl buffer (10 mM Tris-HCl having 100 mM KCl and 0.1 mM EDTA, pH 7.4) followed at 292 nm as a function of temperature. The dashed–dotted curve (at 292 nm) is obtained when the ligand is mixed with a preformed G4DNA and the dashed curve (at 265 nm) is obtained when G4DNA is formed in presence of the ligand (first heated at 90 °C for 5 min and then cooled slowly). (C) Cooling curves of the solutions of Hum_{21} DNA and its complexes with **1b** and **2d**.

Taken together, the CD spectroscopic and electrophoretic mobility shift assay data illustrate how the compounds **1b** and **2d** direct the folding of $d[G_3(T_2AG_3)_3]$ into parallel quadruplex DNA structure when the G4DNA is formed in presence of each

Table 4. Melting Temperatures of the Hum_{21} G4DNA (2 μM) Formed in KCl Buffer (10 mM Tris-HCl having 100 mM KCl and 0.1 mM EDTA) and G4DNA Complexed with 20 μM ([ligand]:[DNA] ratio = 10) of the Indicated Ligands[a,b]

entry	system	T_m °C	ΔT_m °C[a]
1	Hum_{21}	66	
2	Hum_{21} + **1b**	72	6
3	Hum_{21} + **1b**[c]	80.5	14.5
4	Hum_{21} + **2d**	75	9
5	Hum_{21} + **2d**[c]	82	16

[a]Melting temperatures were obtained upon following temperature induced changes in the CD spectral peaks at 292 nm for the preformed G4DNA and at 265 nm for the G4DNA formed in presence of a ligand. The results are average of three experiments and are within ±0.5 °C of each other. [b]ΔT_m values were obtained from the difference in the T_ms of the ligand bound and the uncomplexed G4DNA. [c]For entries 3 and 5, G4DNA was formed in KCl buffer in the presence of indicated ligand (first heated to 90 °C for 5 min and then cooled slowly).

of the above compounds in solution containing K^+ ion. The pharmacophore unit of the compounds might be tightly bound at each binding site to provide the higher stabilization.

Telomerase Inhibition (TRAP Assay). Because telomerase is an important drug target for treating cancers, we have examined each ligand toward its ability to inhibit human telomerase in a modified cell-free telomerase repeat amplification protocol (TRAP) test.[42] Ligands were tested at the concentration ranging from 2.5 to 60 μM for effecting inhibition of the telomerase activity. As expected, dimeric ligands were found to be more potent toward telomerase inhibition than the corresponding monomeric ligands (Figure 9 and Figure S13, Supporting Information). While the monomeric ligand **1b** inhibits the telomerase activity at ~30 μM concentration, the dimeric compound **2d** has inhibited the telomerase activity only at 5 μM concentration (Figure 9). The IC_{50} values for the telomerase inhibition have been determined and are shown in Table 5. Interestingly, **1a** showed a lower IC_{50} value than that of **1b**. Dimeric ligands displayed much lower IC_{50} values than the monomeric ligands.

Cancer Cell-Specific Toxicity. To check the selective toxicity of the synthesized ligands toward cancer cells, we treated **1b** and **2d** with human breast cancer cells (MBA-MD231) and normal human keratinocyte cells (HaCat) for 6 and 48 h using MTT based cell viability assay (Figure 10). Both the ligands showed concentration-dependent cytotoxity toward the cancer cells. In contrast, these ligands were significantly less toxic toward the normal cells. Observation of higher cytotoxicity of the ligands toward the cancer cells over the normal cells may be correlated with their ability to fold the longer telomeric ends (in cancer cells) into the G4DNA and to inhibit telomerase in turn.[3−8] Telomerase is not believed to be active in the normal cells, and hence they were less affected by the ligands.[4,7]

Molecular Modeling. To gain insight into the nature of binding of the monomeric ligand **1b** with the telomeric G4DNA, we adopted an approach that combined molecular docking and MD simulations. The parallel propeller-type X-ray G-quadruplex DNA structure (PDB 1KF1)[12] was a used as template for the modeling studies. The propeller shaped G4DNA structures could be characterized by two external G-quartet planes, the 5′-G-quartet surface is relatively more hydrophobic for favoring π-stacking interactions whereas the 3′-

dx.doi.org/10.1021/jm200860b | J. Med. Chem. 2012, 55, 2981−2993

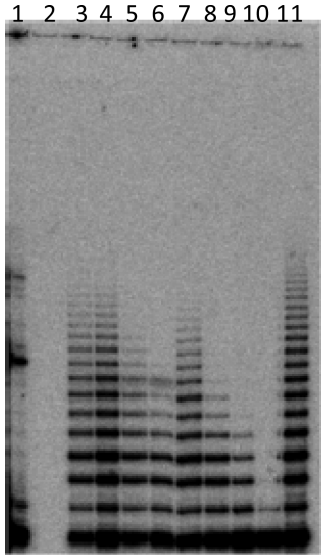

Figure 9. Representative experiments for the determination of the telomerase inhibitory properties by the bisbenzimidazole derivatives. TRAP assay performed with increasing concentrations **1b** and **2d**. Lane 1, (−) ve control (absence of enzyme and ligand); lane 2, R = PCR control; lanes 3, 4, 5, and 6, TRAP reaction mixture + (5, 10, 30, and 60 μM of **1b**); lanes 7, 8, 9, and 10, TRAP reaction mixture + (2.5, 5, 10, and 30 μM of **2d**); lane 11, (+) ve control (absence of the ligand). Note: TRAP assays with more ligands are given in the Supporting Information.

Table 5. IC_{50} Values against Telomerase Found for the Different Ligands[a]

entry	ligand	IC_{50} (μM)
1	**1a**	22.3
2	**1b**	28.0
3	**2a**	10.8
4	**2b**	6.2
5	**2c**	6.0
6	**2d**	5.5

[a]The results are average of three experiments and are within ±1% of each other.

G-quartet surface is more favored for electrostatic interactions, and both the 5′- and 3′- ends are potential binding sites for the above ligands. There are four equivalent phosphate grooves created by three TTA loops on the side, and these are quite deep and easily accessible for the ligands.[12]

Molecular docking studies were first carried out to predict the nature of possible interactions between the ligands and the G4DNA. Previously, it was shown that ligands prefer to stack at the top of the terminal G-tetrads.[43] The intercalation of a ligand in between the successive G-tetrads in a G4DNA is also energetically not favorable.[44] Results from our docking studies suggest that besides having end-stacking interactions, flexible ligands could be readily accommodated in the groove regions of the propeller-type structures.

On the basis of the docking results, we have taken the lowest, final docked energy ligand−G4DNA complexes. Then MD simulations (8 ns) were performed on four complexes formed by the G4DNA (propeller-type) with ligand **1b** in two binding modes (end-stacking and groove-binding). Each model was found to be quite stable during the dynamics runs. Monomeric ligand **1b** was found to stack on the 5′-side. Because of the presence of an easily accessible groove, **1b** also binds to the grooves of the G4DNA, which is also evident from the occurrence of an ICD signal in the CD spectra (Figure 11).

The core phenyl ring and the benzimidazole linkers that form the central pharmacophore of the ligand **1b** interact strongly with the guanine tetrads by maximizing the π-stacking interactions. The planar bisbenzimidazole moiety effectively stacks over the surface of the guanine residues of one side of the G-tetrad (Figure 11). Another possible reason for the strong stabilization potential of these ligands might be because of the comparable size of the bisbenzimidazole core of each ligands with that of the G-quartet.[26,27] Therefore, the molecular feature of the central core (internal hydrogen bonds) and the electronic/electrostatic properties make these ligands almost perfectly suitable for the recognition of the G4DNA. Piperazine substituted side chains go toward the grooves and make hydrogen bonding interactions with the sugar and the phosphate backbones of the G4DNA organization effective. Thus one may hypothesize that the dimeric ligands, particularly the ones having longer flexible linker, would be more effective for the stabilization of telomeric G4DNA.

CONCLUSIONS

In this report, we describe the design and synthesis of six new bisbenzimidazole based ligands which efficiently stabilize the G4DNA assembled from a human DNA telomeric sequence. This occurs in both cases, i.e., with the preformed G4DNA and the G4DNA formed in the presence of each ligand in solution containing various monovalent alkali metal salts. The above ligands direct the folding of telomeric DNA into an unusually stable parallel-stranded conformation (as evident from the CD melting data) when the G4DNA is formed along with the compound in K^+ solution. Dimeric ligands provide significantly higher stabilization to the G4DNA than the corresponding monomeric ligands in both the cases. Recent studies have shown that 48-mer sequence $d(TTAGGG)_8$ forms a dimeric DNA structure containing 2-folded G-quadruplex units.[45] In this context, the dimeric compounds and their multimeric forms, having sufficiently long intervening spacer between each monomeric unit, should be appropriate even for the stabilization of the G4DNA in vivo. The G4DNA structures in human genome may be readily folded and stacked end-to-end to form compact-stacking structures for multimers in the elongated telomeric DNA,[46] and these types of dimeric ligands may bind with two (or more) consecutive G-quadruplex loops. Telomerase inhibition assay reinforces this fact as dimeric ligand (**2d**) inhibits the enzyme at significantly lower concentration compared to its monomeric counterpart (**1b**). We have reported earlier that the monomeric ligands exhibit weak binding with the duplex DNA.[26,27] The dimeric ligand **2d** also shows ∼100-fold higher affinity for the G4DNA than the duplex DNA. Importantly, ligands are selectively more cytotoxic toward cancer cells than normal cells. Higher selectivity toward the cancer cells may be linked with the telomerase inhibition capability of the ligands.

In summary, we have designed a new class of G-quadruplex stabilizing ligands and demonstrated that oligo-oxyethylene linkers of suitable length form a part of a pharmacophore capable of having favorable interactions with the G-tetrads. We have synthesized a first generation of monomers which show excellent affinity and selectivity toward the G-quadruplex. Moreover, we have demonstrated that dimerization of ligands via appropriate choice of linker and its optimal length has

dx.doi.org/10.1021/jm200860b | J. Med. Chem. 2012, 55, 2981−2993

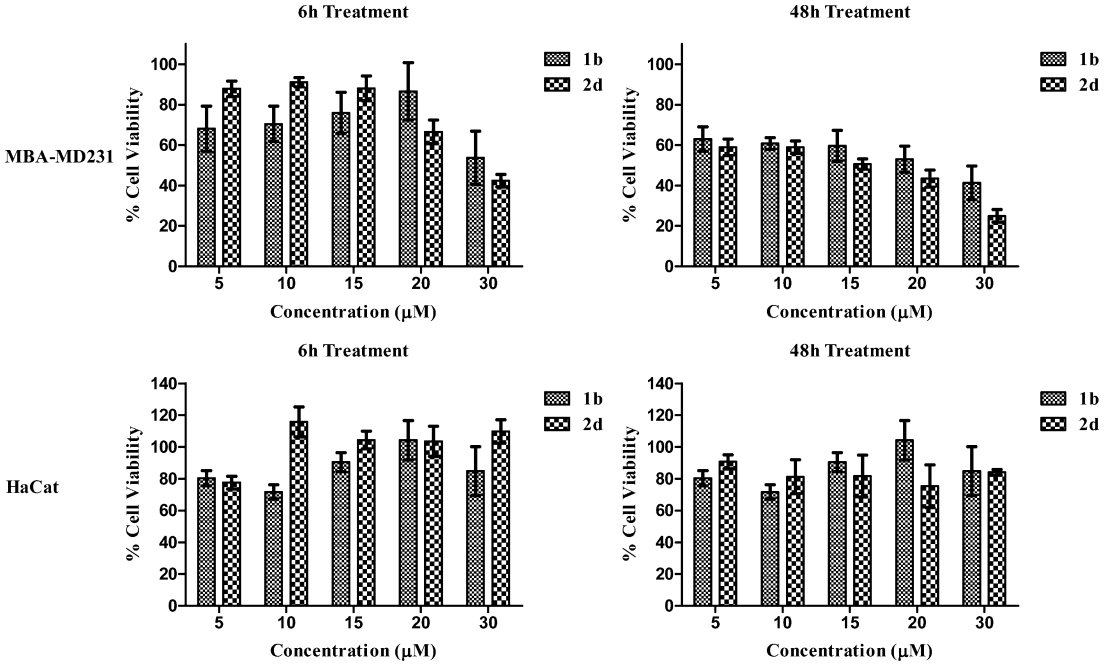

Figure 10. Effect of ligands **1b** and **2d** on the cell viability after short-term exposure (for 6 and 48 h) of human breast cancer cells (MBA-MD231) and normal human keratinocyte cells (HaCat) at specified concentrations as measured by the MTT assay. Each experiment was performed three times and an average at each point is shown.

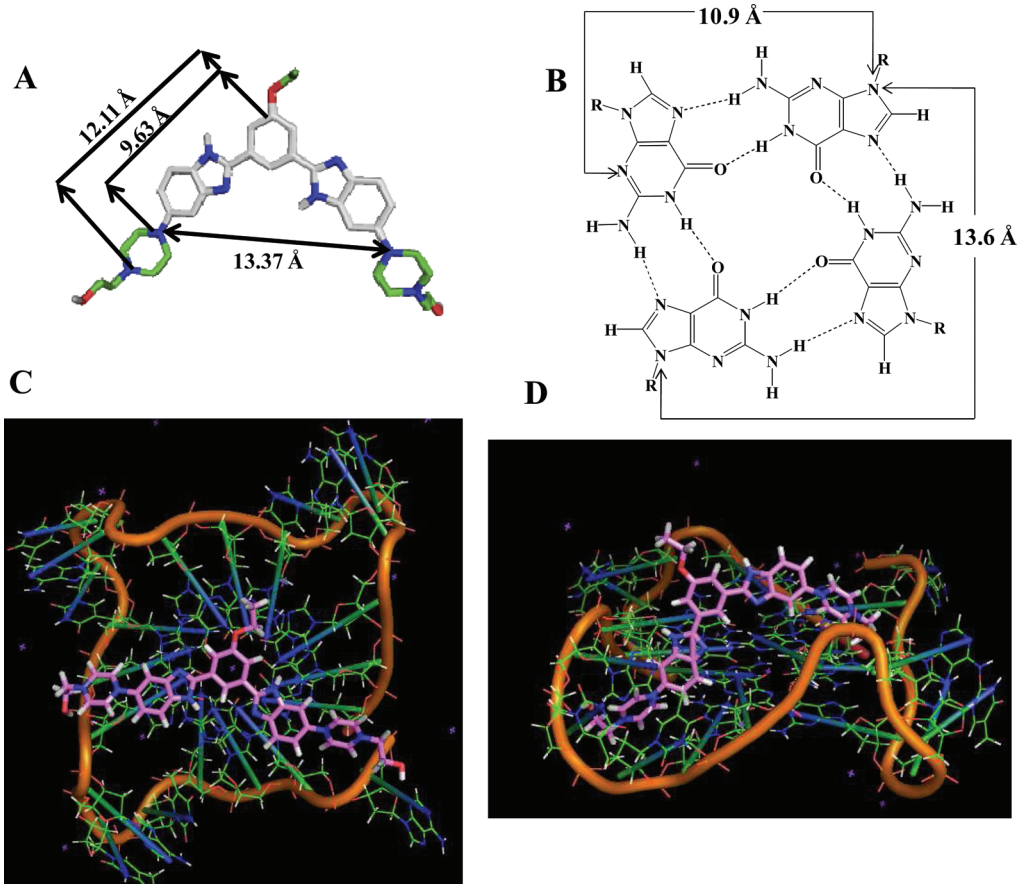

Figure 11. (A) Optimized structure at the B3LYP/6-31G* level of theory of **1b** and (B) chemical structure of the G-tetrad with interatomic distances as given in the crystal structure in ref 12. Simulated structure of the **1b**−G4DNA complex: (C) **1b** stacking on the surface of G-quartet plane at 1:1 ratio. (D) **1b** bound to the groove of the propeller shaped G4DNA. K^+ ions that come from the bulk solution, stabilize the complex during dynamic run, are shown by purple stars. Ligand is shown in "sticks" model colored by atom type (purple−white). Propeller shaped G4DNA is represented as a cartoon form (green−orange).

dx.doi.org/10.1021/jm200860b | *J. Med. Chem.* 2012, 55, 2981−2993

applicability and relevance in the field of G-quadruplex ligand discovery. These findings should spearhead a new modular approach for the identification and synthetic attainment of lead structures, analogues, and modification of existing quadruplex binders. This strategy should lead to increased diversity and, in turn, selectivity and potency necessary for the anticancer drug design.

MATERIALS AND METHODS

Materials and General Spectroscopic Characterizations. See Supporting Information. All tested ligands were found to be at least >95% pure by elemental analysis (Table S1, Supporting Information).

Synthesis. Synthesis of precursors (**5**−**12**) has been described in the Supporting Information.

*General Method for the Synthesis of 1,3-Phenylene-bis-(piperazinyl benzimidazole) Derivatives (**2a**−**2d**).* To a freshly prepared ethanolic solution of either 4-(4-methylpiperazin-1-yl)-benzene-1,2-diamine (**13**)[27] or 4-[4-(2-hydroxyethyl)piperazin-1-yl]-benzene-1,2-diamine (**14**),[27] 1/4th equivalent of the appropriate tetraaldehyde (either **11** or **12**, Supporting Information) was added, and to this solution, two equivalents of sodium metabisulphite ($Na_2S_2O_5$) dissolved in minimum quantity of water was added. The resulting reaction mixture was refluxed for 8 h with stirring, then cooled to room temperature, and finally filtered through Celite. Ethanol was then removed from the reaction mixture under reduced pressure to obtain a residue. This material was then purified by column chromatography (EtOAc/MeOH) on silica gel (70−220 mesh size) to obtain the required product as given in the following.

*1,8-Bis-[2,2′-(5-phenoxy-1,3-phenylene)-bis[5-(4-methyl-1-piperazinyl)-1H-benzimidazole]]-3,6-dioxo-octane (**2a**).* Freshly prepared 4-(4-methylpiperazin-1-yl)-benzene-1,2-diamine (**13**, 165 mg, 0.8 mmol) and **11** (83 mg, 0.2 mmol) and $Na_2S_2O_5$ (75 mg, 1.6 mmol) were reacted as per the general protocol. Isolated yield 138 mg, 60%; mp 287−288 °C. IR: 3356, 2956, 2835, 2729, 1633, 1455, 1223 cm^{-1}. ^1H NMR (DMSO-d_6) δ 13.2 (bs, 4H), 7.9 (bs, 4H), 7.6 (bs, 6H), 7.0 (bs, 8H), 4.3 (bs, 4H), 3.7 (bs, 24H), 3.05 (bs, 16H), 2.65 (bs, 12 H). ^{13}C NMR (DMSO-d_6) δ: 159.29, 149.31, 147.4, 141.5, 139.6, 136.0, 132.2, 128.16, 118.9, 116.8, 114.5, 113.7, 111.2, 105.3, 103.0, 97.3, 69.0, 67.5, 58.13, 53.9, 49.5, 48.8, 42.28. m/z (MALDI-TOF) found, 1159.610 (calcd, 1159.609, $[M + H]^+$). Anal. (calcd for $C_{66}H_{78}N_{16}O_4 \cdot H_2O$): C, 67.32; H, 6.85; N, 19.03. Found: C, 67.25; H, 6.87; N, 18.95.

*1,8-Bis-[2,2′-(5-phenoxy-1,3-phenylene)-bis[5-(4-(2-hydroxyethyl)-1-piperazinyl)-1H-benzimid-azole]-3,6-dioxo-octane (**2b**).* Freshly prepared 4-[4-(2-hydroxyethyl)-piperazin-1-yl]-benzene-1,2-diamine (**14**, 188 mg, 0.8 mmol) and **11** (83 mg, 0.2 mmol) and $Na_2S_2O_5$ (75 mg, 1.6 mmol) were reacted as per the general protocol given above. Isolated yield 158 mg, 62%; mp > 290 °C. IR: 3404, 3019, 2870, 1634, 1570, 1456, 1218 cm^{-1}. ^1H NMR (DMSO-d_6) δ 13.2 (bs, 4H), 7.9 (bs, 4H), 7.5 (m, 6H), 7.0 (bs, 8H), 4.25 (bs, 4H), 3.72 (bs, 20H), 3.15 (bs, 16H), 2.6 (bs, 24 H). ^{13}C NMR (DMSO-d_6) δ: 159.31, 149.35, 143.7, 142.1, 141.7, 139.8, 136.1, 128.16, 120.4, 113.5, 107.5, 103.1, 97.1, 70.0, 67.6, 59.95, 58.15, 53.1, 49.60, 48.02, 42.68. m/z (MALDI-TOF) found, 1279.705 (calcd, 1279.682, $[M + H]^+$). Anal. (calcd for $C_{70}H_{86}N_{16}O_8 \cdot 2H_2O$): C, 63.91; H, 6.90; N, 17.04. Found: C, 63.78; H, 6.92; N, 16.93.

*1,11-Bis-[2,2′-(5-phenoxy-1,3-phenylene)-bis[5-(4-methyl-1-piperazinyl)-1H-benzimidazole]]-3,6,9-trioxo-undecane (**2c**).* Freshly prepared 4-(4-methylpiperazin-1-yl)-benzene-1,2-diamine (**13**, 165 mg, 0.8 mmol) and **12** (91 mg, 0.2 mmol) and $Na_2S_2O_5$ (75 mg, 1.6 mmol) were reacted as per the general protocol given above. Isolated yield 146 mg, 61%; mp 285−286 °C. IR: 3352, 2959, 2838.5, 2730, 1630, 1450.5, 1227 cm^{-1}. ^1H NMR (DMSO-d_6) δ 11.4 (bs, 4H), 8.0 (bs, 4H), 7.5 (m, 6H), 7.0 (bs, 8H), 4.3 (bs, 4H), 3.8 (bs, 28H), 3.2 (bs, 16H), 2.9 (bs, 12 H). ^{13}C NMR (DMSO-d_6) δ: 159.31, 158.8, 150.2, 148.44, 147.34, 139.12, 129.33, 129.06, 116.95, 115.50, 99.89, 99.12, 79.22, 69.88, 68.78, 67.93, 52.11, 49.02, 46.54, 41.83. m/z (MALDI-TOF) found, 1203.892 (calcd, 1203.894, $[M + H]^+$). Anal. (calcd for $C_{68}H_{82}N_{16}O_5 \cdot 1.5H_2O$): C, 67.25; H, 7.05; N, 18.45. Found: C, 67.12; H, 6.95; N, 18.42.

*1,11-Bis-[2,2′-(5-phenoxy-1,3-phenylene)-bis[5-(4-(2-hydroxyethyl)-1-piperazinyl)-1H-benzimidazole]]-3,6,9-trioxo-undecane (**2d**).* Freshly prepared 4-[4-(2-hydroxyethyl)-piperazin-1-yl]-benzene-1,2-diamine (**14**, 188 mg, 0.8 mmol) and **12** (91 mg, 0.2 mmol) and $Na_2S_2O_5$ (75 mg, 1.6 mmol) were reacted as per the general protocol given above. Isolated yield 163 mg, 62%; mp > 290 °C. IR: 3410, 3016, 2878, 1614, 1565, 1450, 1220 cm^{-1}. ^1H NMR (DMSO-d_6) δ 13.1 (bs, 4H), 7.85 (bs, 4H), 7.5 (bs, 6H), 7.0 (bs, 8H), 4.3 (bs, 4H), 3.8 (bs, 12H), 3.68 (bs, 16H), 3.58 (bs, 24H), 3.2 (bs, 16 H). ^{13}C NMR (DMSO-d_6) δ: 159.19, 158.79, 150.24, 146.50, 132.09, 119.53, 116.95, 115.50, 114.24, 113.01, 79.24, 69.83, 68.86, 67.72, 57.88, 55.4, 51.51, 47.06, 42.0. m/z (MALDI-TOF) found, 1323.975 (calcd, 1323.978, $[M + H]^+$). Anal. (calcd for $C_{72}H_{90}N_{16}O_9 \cdot 1.5H_2O$): C, 64.03; H, 6.94; N, 16.59. Found: C, 63.98; H, 7.0; N, 16.5.

Oligonucleotides. HPLC purified oligodeoxyribonucleotides (ODNs) d[$G_3(T_2AG_3)_3$], abbreviated as Hum_{21}, and d[T_{20}] were purchased from Sigma Genosys, Bangalore. Their purity was confirmed using high resolution sequencing gel. The molar concentration of each ODN was determined from absorbance measurements at 260 nm based on their molar extinction coefficients (ε_{260}) 215000 and 148400, respectively, for d[$G_3(T_2AG_3)_3$] and d[T_{20}], respectively.

G-Quadruplex Formation, Circular Dichroism Spectroscopy, T_m Studies, Fluorescence Spectroscopy, UV−Vis Titrations, Polyacrylamide Gel Electrophoresis, Telomerase Assay, and Computational Studies. These studies have been performed as described in our earlier reports.[26,27]

Cell Viability Assay. Human breast cancer cells (MBA-MD231) and normal human keratinocyte cells (HaCat) were seeded in 96-well plates (15.0×10^3/well). Cells were grown for 24 h before treatment to get >70% confluency and exposed to various concentrations of ligands in presence of 0.2% FBS. After either 6 or 48 h incubation at 37 °C in a humidified atmosphere of 5% CO_2, old medium was replaced with the new one containing 10% FBS in DMEM and cells were further grown for 42 h post treatment. Then 20 μL of 5 mg/mL methyl thiazolyl tetrazolium (MTT) reagent was added to 200 μL of the medium present in each well, and cells were further incubated for 4 h. Old medium was discarded, and formazan crystals were dissolved in DMSO and reading (fluorescence intensity, FI) was taken at 595 nm in the ELISA plate reader. All ligand doses were parallel tested in triplicate. Percentage cell viability was calculated by using the formula,

$$\%\text{cell viability} = [(\text{FI}_{(595)}\text{of treated cells} - \text{FI}_{(595)}\text{of plain DMSO}) / (\text{FI}_{(595)}\text{of untreated cells} - \text{FI}_{(595)}\text{of plain DMSO})] \times 100$$

ASSOCIATED CONTENT

Supporting Information

Synthesis of the precursors for the dimeric ligands, NMR spectra of the key compounds, additional CD and fluorescence data, computational results, CD melting curves, topology change in Hum21 by electrophoresis, additional TRAP assays of ligands. This material is available free of charge via the Internet at http://pubs.acs.org.

AUTHOR INFORMATION

Corresponding Author

*Phone: (91)-80-22932664. Fax: (91)-80-22930529. E-mail: sb@orgchem.iisc.ernet.in.

Notes

The authors declare no competing financial interest.

Note: "preformed" G-quadruplex DNA refers to the G-quadruplex DNA formed in absence of any added ligand (i.e., the unstructured DNA is *annealed* in the chosen buffer, having indicated salt, however, with no added ligand). [ligand]:[DNA] ratio = equiv of ligand (μM) with respect to that of DNA (μM of DNA strand). [DNA]:[ligand] ratio = equiv of DNA (μM of DNA strand) with respect to that of ligand (μM).

■ ACKNOWLEDGMENTS

This work was supported by a grant (J.C. Bose Fellowship grant to Prof. S. Bhattacharya) from the Department of Science and Technology (DST), New Delhi, India. A.K.J. is thankful to DST for a grant as a Fast Track Project and DBT New Delhi for a postdoctoral fellowship. We thank Santosh K. Misra for technical assistance.

■ ABBREVIATIONS USED

G4DNA, G-quadruplex DNA; ODN, oligodeoxynucleotide; CD, circular dichroism; ICD, induced circular dichorism; PEG, polyethylene glycol; TRAP, telomerase repeat amplification protocol; FI, fluorescence intensity; EDTA, ethylenediaminetetraacetic acid; MTT, methyl thiazolyl tetrazolium; DMSO, dimethyl sulphoxide; NMR, nuclear magnetic resonance; MALDI, matrix assisted laser desorption ionization; IR, infrared

■ REFERENCES

(1) Meyne, J.; Ratliff, R. L.; Moyzis, R. K. Conservation of the human telomere sequence $(TTAGGG)_n$ among vertebrates. *Proc. Natl. Acad. Sci. U.S.A.* **1989**, *86*, 7049−7053.

(2) Yu, H.-Q.; Miyoshi, D.; Sugimoto, N. Characterization of structure and stability of long telomeric DNA G-quadruplexes. *J. Am. Chem. Soc.* **2006**, *128*, 15461−15468.

(3) Blackburn, E. H. Structure and function of telomeres. *Nature* **1991**, *350*, 569−573.

(4) (a) Franceschin, M. J. G-Quadruplex DNA structures and organic chemistry: more than one connection. *Eur. J. Org. Chem.* **2009**, 2225−2238. (b) Jain, A. K.; Bhattacharya, S. Interaction of G-quadruplexes with nonintercalating DNA minor groove binding ligands. *Bioconjugate Chem.* **2011**, *22*, 2355−2368. (c) Jain, A. K.; Bhattacharya, S. Recent developments in the chemistry and biology of G-quadruplexes with reference to the DNA groove binders. *Curr. Pharm. Des.* **2012**, *18*, 1900−1916. (d) Folini, M.; Venturini, L.; Cimino-Reale, G.; Zaffaroni, N. Telomeres as targets for anticancer therapies. *Expert Opin. Ther. Targets* **2011**, *15*, 579−593.

(5) McEachern, M. J.; Krauskopf, A.; Blackburn, E. H. Telomers and their control. *Annu. Rev. Genet.* **2000**, *34*, 331−358.

(6) Harley, C. B.; Futcher, A. B.; Greider, C. W. Telomeres shorten during ageing of human fibroblasts. *Nature* **1990**, *345*, 458−460.

(7) Wright, W. E.; Tesmer, V. M.; Huffman, K. E.; Levene, S. D.; Shay, J. W. Normal human chromosomes have long G-rich telomeric overhangs at one end. *Genes Dev.* **1997**, *11*, 2801−2809.

(8) (a) Gowan, S. M.; Harrison, J. R.; Patterson, L.; Valneti, M.; Read, M. A.; Neidle, S.; Kelland, L. R. A G-quadruplex-interactive potent small-molecule inhibitor of telomerase exhibiting in vitro and in vivo antitumor activity. *Mol. Pharmacol.* **2002**, *61*, 1154−1162. (b) Chakraborty, T. K.; Arora, A.; Roy, S.; Kumar, N.; Maiti, S. Furan based cyclic oligopeptides selectively target G-quadruplex. *J. Med. Chem.* **2007**, *50*, 5539−5542.

(9) Cech, T. R. Life at the end of chromosome: telomers and telomerase. *Angew. Chem., Int. Ed.* **2000**, *39*, 34−43.

(10) Alberts, B.; Johnson, A.; Lewis, J.; Raff, M.; Roberts, K.; Walter, P., *Molecular Biology of the Cell*, 4th ed.; Garland Science: New York, 2002.

(11) Wang, Y.; Patel, D. J. Solution structure of the human telomeric repeat $d[AG_3(T_2AG_3)_3]$ G-tetraplex. *Structure* **1993**, *1*, 263−282.

(12) Parkinson, G. N.; Lee, M. P.; Neidle, S. Crystal structure of parallel quadruplexes from human telomeric DNA. *Nature* **2002**, *417*, 876−880.

(13) (a) Ambrus, A.; Chen, D.; Dai, J.; Bialis, T.; Jones, R. A.; Yang, D. Human telomeric sequence forms a hybrid-type intramolecular G-quadruplex structure with mixed parallel/antiparallel strands in potassium solution. *Nucleic Acids Res.* **2006**, *34*, 2723−2735. (b) Xu, Y.; Noguchi, Y.; Sugiyama, H. The new models of the human telomere d $[AGGG(TTAGGG)_3]$ in K^+ solution. *Bioorg. Med. Chem.* **2006**, *14*, 5584−5591. (c) Luu, K. N.; Phan, A. T.; Kuryavyi, V.; Lacroix, L.; Patel, D. J. Structure of the human telomere in K^+ solution: an intramolecular (3 + 1) G-quadruplex scaffold. *J. Am. Chem. Soc.* **2006**, *128*, 9963−9970. (d) Yang, D.; Okamoto, K. Structural insights into G-quadruplexes: towards new anticancer drugs. *Future Med. Chem.* **2010**, *2*, 619−646.

(14) Li, J.; Correia, J. J.; Wang, L.; Trent, J. O.; Chaires, J. B. Not so crystal clear: the structure of the human telomere G-quadruplex in solution differs from that present in a crystal. *Nucleic Acids Res.* **2005**, *33*, 4649−4659.

(15) Lim, K. W.; Amrane, S.; Bouaziz, S.; Xu, W.; Mu, Y.; Patel, D. J.; Luu, K. N.; Phan, A, T. Structure of the human telomere in K^+ solution: a stable basket-type G-quadruplex with only two G-tetrad layers. *J. Am. Chem. Soc.* **2009**, *131*, 4301−4309.

(16) Xue, Y.; Kan, Z.; Wang, Q.; Yao, Y.; Liu, J.; Hao, Y.; Tan, Z. Human telomeric DNA forms parallel-stranded intramolecular G-quadruplex in K^+ solution under molecular crowding condition. *J. Am. Chem. Soc.* **2007**, *129*, 11185−11191.

(17) (a) Miyoshi, D.; Sugimoto, N. Molecular crowding effects on structure and stability of DNA. *Biochimie* **2008**, *90*, 1040−1051. (b) Miller, M. C.; Buscaglia, R.; Chaires, J. B.; Lane, A. N.; Trent, J. O. Hydration is a major determinant of the G-quadruplex stability and conformation of the human telomere 3′ sequence of $d(AG_3(TTAG_3)_3$. *J. Am. Chem. Soc.* **2010**, *132*, 17105−17107.

(18) (a) Rodriguez, R.; Pantos, G. D.; Goncalves, D. P. N; Sanders, J. K. M.; Balasubramanian, S. Ligand-driven G-quadruplex conformational switching by using an unusual mode of interaction. *Angew. Chem., Int. Ed.* **2007**, *46*, 5405−5407. (b) Antonio, M. D.; Doria, F.; Richter, S. N.; Bertipaglia, C.; Mella, M.; Sissi, C.; Palumbo, M.; Freccero, M. Quinone methides tethered to naphthalene diimides as selective G-quadruplex alkylating agents. *J. Am. Chem. Soc.* **2009**, *131*, 13132−13141. (c) Tan, J.-H.; Ou, T.-M.; Hou, J.-Q.; Lu, Y.-J.; Huang, S.-L.; Luo, H.-B.; Wu, J.-Y.; Huang, Z.-S.; Wong, K.-Y.; Gu, L.-Q. Isaindigotone derivatives: a new class of highly selective ligands for telomeric G-quadruplex DNA. *J. Med. Chem.* **2009**, *52*, 2825−2835.

(19) (a) Han, H.; Hurley, L. H. G-quadruplex DNA: a potential target for anti-cancer drug design. *Trends Pharmacol. Sci.* **2000**, *21*, 136−142. (b) Kieltyka, R.; Fakhoury, J.; Moitessier, N.; Sleiman, H. F. Platinum phenanthroimidazole complexes as G-quadruplex DNA selective binders. *Chem.—Eur. J.* **2008**, *14*, 1145−1154. (c) Dixon, I. M.; Lopez, F.; Tejera, A. M.; Esteve, J.-P.; Blasco, M. A.; Pratviel, G.; Meunier, B. A G-Quadruplex ligand with 10000-fold selectivity over duplex DNA. *J. Am. Chem. Soc.* **2007**, *129*, 1502−1503. (d) Cian, A. D.; DeLemos, E.; Mergny, J.-L.; Teulade-Fichou, M.-P.; Monchaud, D. Highly efficient G-quadruplex recognition by bisquinolinium compounds. *J. Am. Chem. Soc.* **2007**, *129*, 1856−1857. (e) Alcaro, S.; Artese, A.; Iley, J. N.; Maccari, R.; Missailidis, S.; Ortuso, F.; Ottana, R. Patricia Ragazzon, P.; Vigorita, M. G. Tetraplex DNA specific ligands based on the fluorenone-carboxamide scaffold. *Bioorg. Med. Chem. Lett.* **2007**, *17*, 2509−2514. (f) Ou, T.-M.; Lu, Y.-J.; Zhang, C.; Huang, Z.-S.; Wang, X.-D.; Tan, J.-H.; Chen, Y.; Ma, D.-L.; Wong, K.-Y.; Tang, J. C-O.; Chan, A. S-C.; Gu, L.-Q. Stabilization of G-quadruplex DNA and down-regulation of oncogene *c-myc* by quindoline derivatives. *J. Med. Chem.* **2007**, *50*, 1465−1474.

(20) (a) Maiti, S.; Chaudhury, N. K.; Chowdhury, S. Hoechst 33258 binds to G-quadruplex in the promoter region of human c-myc. *Biochem. Biophys. Res. Commun.* **2003**, *310*, 505−512. (b) Phan, A. T.; Kuryavyi, V.; Gaw, H. Y.; Patel, D. J. Small-molecule interaction with a five-guanine-tract G-quadruplex structure from the human MYC promoter. *Nature Chem. Biol.* **2005**, *1*, 167−173.

(21) Chen, Z.; Zheng, K-w.; Hao, Y-h.; Tan, Z. Reduced or diminished stabilization of the telomere G-quadruplex and inhibition of telomerase by small chemical ligands under molecular crowding condition. *J. Am. Chem. Soc.* **2009**, *131*, 10430−10438.
(22) (a) Jain, A. K.; Tawar, U.; Gupta, S. K.; Dogra, S. K.; Tandon, V. Benzimidazoles: a minor groove-binding ligand-induced stabilization of triple helix. *Oligonucleotides* **2009**, *19*, 53−62. (b) Jain, A. K.; Bhattacharya, S. Groove binding ligands for the interaction with parallel-stranded *ps*-duplex DNA and triplex DNA. *Bioconjugate Chem.* **2010**, *21*, 1389−1403.
(23) (a) Chaudhauri, P.; Majumder, H. K.; Bhattacharya, S. Synthesis, DNA binding, and *leishmania* topoisomerase inhibition activities of a novel series of anthra[1,2-*d*]imidazole-6,11-dione derivatives. *J. Med. Chem.* **2007**, *50*, 2536−2540. (b) Chaudhauri, P.; Ganguly, B.; Bhattacharya, S. An experimental and computational analysis on the differential role of the potential isomers of symmetric bis-2-(pyridyl)1*H*-benzimidazoles as DNA binding agents. *J. Org. Chem.* **2007**, *72*, 1912−1923.
(24) Fu, Y-Te; Keppler, B. R.; Soares, J.; Jarstfer, M. B. BRACO19 analog dimers with improved inhibition of telomerase and hPot 1. *Bioorg. Med. Chem.* **2009**, *17*, 2030−2037.
(25) Iida, K.; Tera, M.; Hirokawa, T.; Shin-ya, K.; Nagasawa, K. G-quadruplex recognition by macrocyclic hexaoxazole (6OTD) dimer: greater selectivity than monomer. *Chem. Commun.* **2009**, 6481−6483.
(26) Bhattacharya, S.; Chaudhuri, P.; Jain, A. K.; Paul, A. Symmetrical bisbenzimidazoles with benzenediyl spacer: the role of the shape of the ligand on the stabilization and structural alterations in telomeric G-quadruplex DNA and telomerase inhibition. *Bioconjugate Chem.* **2010**, *21*, 1148−1159.
(27) Jain, A. K.; Reddy, V. V.; Paul, A.; Muniyappa, K.; Bhattacharya, S. Synthesis and evaluation of a novel class of G-quadruplex-stabilizing small molecules based on the 1,3-phenylene-bis(piperazinyl benzimidazole) system. *Biochemistry* **2009**, *48*, 10693−10704.
(28) (a) Stokke, T.; Steen, H. B. Multiple binding modes for Hoechst 33258 to DNA. *J. Histochem. Cytochem.* **1985**, *33*, 333−338. (b) Tawar, U.; Jain, A. K.; Dwarakanath, B. S.; Chandra, R.; Singh, Y.; Chaudhury, N. K.; Khaitan, D.; Tandon, V. Influence of phenyl ring disubstitution on bisbenzimidazole and terbenzimidazole cytotoxicity: synthesis and biological evaluation as radioprotectors. *J. Med. Chem.* **2003**, *46*, 3785−3792. (c) Tawar, U.; Jain, A. K.; Chandra, R.; Singh, Y.; Dwarakanath, B. S.; Chaudhury, N. K.; Good, L.; Tandon, V. Minor groove binding DNA ligands with expanded A/T sequence length recognition, selective binding to bent DNA regions and enhanced fluorescent properties. *Biochemistry* **2003**, *42*, 13339−13346. (d) Bhattacharya, S.; Chaudhuri, P. Medical implications of benzimidazole derivatives as drugs designed for targeting DNA and DNA associated processes. *Curr. Med. Chem.* **2008**, *15*, 1762−1777. (e) Paul, A.; Bhattacharya, S. Chemistry and biology of DNA-binding small molecules. *Curr. Sci.* **2012**, *102*, 212−231.
(29) (a) Dash, J.; Shirude, P. S.; Balasubramanian, S. G-quadruplex recognition by bis-indole carboxamides. *Chem. Commun.* **2008**, 3055−3057. (b) Li, G.; Huang, J.; Zhang, M.; Zhou, Y.; Zhang, D.; Wu, Z.; Wang, S.; Weng, X.; Zhou, X.; Yang, G. Bis(benzimidazole)pyridine derivative as a new class of G-quadruplex inducing and stabilizing ligands. *Chem. Commun.* **2008**, 4564−4566.
(30) (a) Sheftel, V. O. In *Indirect Food Additives and Polymers: Migration and Toxicology*; CRC: Boca Raton, FL, 2000; p 1114. (b) Corpet, D. E.; Parnaud, G.; Delverdier, M.; Peiffer, G.; Tache, S. Consistent and fast inhibition of colon carcinogenesis by polyethylene glycol in mice and rats given various carcinogens. *Cancer Res.* **2000**, *60*, 3160−3164.
(31) Jain, A. K.; Awasthi, S. K.; Tandon, V. Triple helix stabilization by covalently linked DNA−bisbenzimidazole conjugate synthesized by maleimide-thiol coupling chemistry. *Bioorg. Med. Chem.* **2006**, *14*, 6444−6452.
(32) Cian, A.; De.; Guittat, L.; Kaiser, M.; Sacca, B.; Amrane, S.; Bourdoncle, A.; Albertti, P.; Teulade-Fichou, M.-P.; Lacriox, L.; Mergny, J.-L. Fluorescence-based melting assays for studying quadruplex ligands. *Methods* **2007**, *42*, 183−195.
(33) Xu, L.; Zhang, D.; Huang, J.; Deng, M.; Zhang, M.; Zhou, X. High fluorescence selectivity and visual detection of G-quadruplex structures by a novel dinuclear ruthenium. *Chem. Commun.* **2010**, *46*, 743−745.
(34) Yang, D.-Y.; Chang, T.-C.; Sheu, S.-Y. Interaction between human telomere and a carbazole derivative: a molecular dynamics simulation of a quadruplex stabilizer and telomerase inhibitor. *J. Phys. Chem. A* **2007**, *111*, 9224−9232.
(35) Campbell, N. H.; Parkinson, G. N.; Reszka, A. P.; Neidle, S. Structural basis of DNA quadruplex recognition by an acridine drug. *J. Am. Chem. Soc.* **2008**, *130*, 6722−6724.
(36) (a) Kaushik, M.; Kukreti, S. Temperature induced hyperchromism exhibited by Hoechst 33258: evidence of drug aggregation from UV-melting method. *Spectrochim. Acta, Part A* **2003**, *59*, 3123−3129. (b) Kobayashi, M.; Kusakawa, T.; Saito, M.; Kaji, S.; Oomura, S.; Morita, Y.; Hasan, Q.; Tamiya, E. Electrochemical DNA quantification based on aggregation induced by Hoechst 33258. *Electrochem. Commun.* **2004**, *6*, 337−343.
(37) (a) Miyoshi, D.; Matsumura, S.; Nakano, S.; Sugimoto, N. Duplex dissociation of telomere DNAs induced by molecular crowding. *J. Am. Chem. Soc.* **2004**, *126*, 165−169. (b) Oganesian, L.; Moon, I. K.; Bryan, T. M.; Jarstfer, M. B. Extension of G-quadruplex DNA by ciliate telomerase. *EMBO J.* **2006**, *25*, 1148−1159.
(38) Franceschin, M.; Rossetti, L.; Ambrosio, A. D.; Schirripa, S.; Bianco, A.; Ortaggi, G.; Savino, M.; Schults, C.; Neidle, S. Natural and synthetic G-quadruplex interactive berberine derivatives. *Bioorg. Med. Chem. Lett.* **2006**, *16*, 1707−1711.
(39) Gomez, D.; Paterski, R.; Lemarteleur, T.; Shin-ya, K.; Mergny, J.-L.; Riou, J.-F. Interaction of telomestatin with the telomeric single-strand overhang. *J. Biol. Chem.* **2004**, *279*, 41487−41494.
(40) Clark, G. R.; Pytel, P. D.; Squire, C. I.; Neidle, S. Structure of the first parallel DNA quadruplex−drug complex. *J. Am. Chem. Soc.* **2003**, *125*, 4066−4066.
(41) Huang, H.-S.; Chon, C.-L.; Guo, C.-L.; Yuan, C.-L.; Lu, Yu-C.; Shieh, Fu-Y.; Liu, J.-J. Human telomerase inhibition and cytotoxicity of regioisomeric disubstituted amidoanthraquinones and aminoanthraquinones. *Bioorg. Med. Chem.* **2005**, *13*, 1435−1444.
(42) Kim, N. W.; Wu, F. Advances in quantification and characterization of telomerase activity by the telomeric repeat amplification protocol (TRAP). *Nucleic Acids Res.* **1997**, *25*, 2595−2597.
(43) (a) Haider, S. M.; Parkinson, G. N.; Neidle, S. Structure of a G-quadruplex−ligand complex. *J. Mol. Biol.* **2003**, *326*, 117−125. (b) Parkinson, G. N.; Ghosh, R.; Neidle, S. Structural basis for binding of porphyrin to human telomeres. *Biochemistry* **2007**, *46*, 2390−2397.
(44) Read, M. A.; Neidle, S. Structural characterization of a guanine−quadruplex ligand complex. *Biochemistry* **2000**, *39*, 13422−13432.
(45) (a) Petraccone, L.; Trent, J. O.; Chaires, J. B. The tail of the telomere. *J. Am. Chem. Soc.* **2008**, *130*, 16530−16532. (b) Pedroso, I. M.; Duarte, L. F.; Yanez, G.; Burkewitz, K.; Fletcher, T. M. Sequence specificity of inter- and intramolecular G-quadruplex formation by human telomeric DNA. *Biopolymers* **2007**, *87*, 74−84.
(46) (a) Dai, J.; Carver, M.; Punchihewa, C.; Jones, R. A.; Yang, R. A.; G-quadruplex, D. induced stabilization by 2′-deoxy-2′-fluoro-D-arabinonucleic acids (2′ F-ANA). *Nucleic Acids Res.* **2007**, *35*, 4927−4988. (b) Haider, S.; Parkinson, G. N.; Neidle., S. Molecular dynamics and principal components analysis of human telomeric quadruplex multimers. *Biophys. J.* **2008**, *95*, 296−311.